

## Supporting Information

### Self-assembly of carboxylated polythiophene nanowires for improved bulk heterojunction morphology in polymer solar cells

Weiwei Li,<sup>a,b,§</sup> Brian J. Worfolk,<sup>a,b,§</sup> Peng Li,<sup>b</sup> Tate C. Hauger,<sup>a,b</sup> Kenneth D. Harris<sup>b</sup> and Jillian M. Buriak<sup>\*a,b</sup>

<sup>a</sup> Department of Chemistry, University of Alberta, Edmonton, Alberta, T6G 2G2, Canada.

E-mail: jburiak@ualberta.ca

<sup>b</sup> National Institute for Nanotechnology, 11421 Saskatchewan Drive, Edmonton, Alberta, T6G 2M9, Canada.

<sup>§</sup> These two authors have equally contributed to this study.

#### Surface Energy Calculation:

The method to calculate the surface energy relies on the following set of equations:<sup>S1</sup>

$$1 + \cos \theta = 2\sqrt{\gamma_s^d} \left( \frac{\sqrt{\gamma_l^d}}{\gamma_l^v} \right) + 2\sqrt{\gamma_s^h} \left( \frac{\sqrt{\gamma_l^h}}{\gamma_l^v} \right) \quad (1)$$

$$\gamma_s = \gamma_s^d + \gamma_s^h \quad (2)$$

In these equations, the indices h and d refer to the hydrogen bonding and dispersion force components, while s and l denote solid or liquid.  $\gamma_s$  refers to the surface energy of the solid,  $\gamma_l^v$  is the surface energy of the liquid, and  $\theta$  is the contact angle of the liquid with the solid surface. The surface energy parameters were found tabulated in the literature,<sup>S2</sup> and the relevant values are listed below:

	$\gamma_l^d$ (mJ/m <sup>2</sup> )	$\gamma_l^h$ (mJ/m <sup>2</sup> )	$\gamma_l^v$ (mJ/m <sup>2</sup> )
H <sub>2</sub> O	21.8	51.0	72.8
n-hexadecane	26.35	0	26.35

To determine  $\gamma_s$ , we substitute the measured contact angle and known parameters  $\gamma_l^d$ ,  $\gamma_l^h$  and  $\gamma_l^v$  into equation (1) for both H<sub>2</sub>O and *n*-hexadecane as solvents. This forms a system of two equations in two unknowns that may be solved to calculate  $\gamma_s^d$  and  $\gamma_s^h$ . Equation (2) is then invoked to determine  $\gamma_s$ .

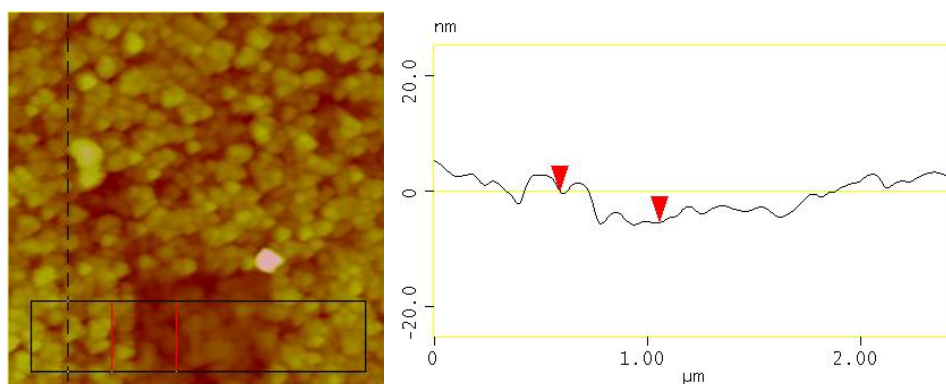


**Fig. S1** Determination by AFM of the thickness of P3CPenT deposited onto an ITO surface using the solution absorption method. The average thickness measured by this technique is ~4 nm. The red triangles were generated in the AFM analysis software, but were not used in the determination of thickness.

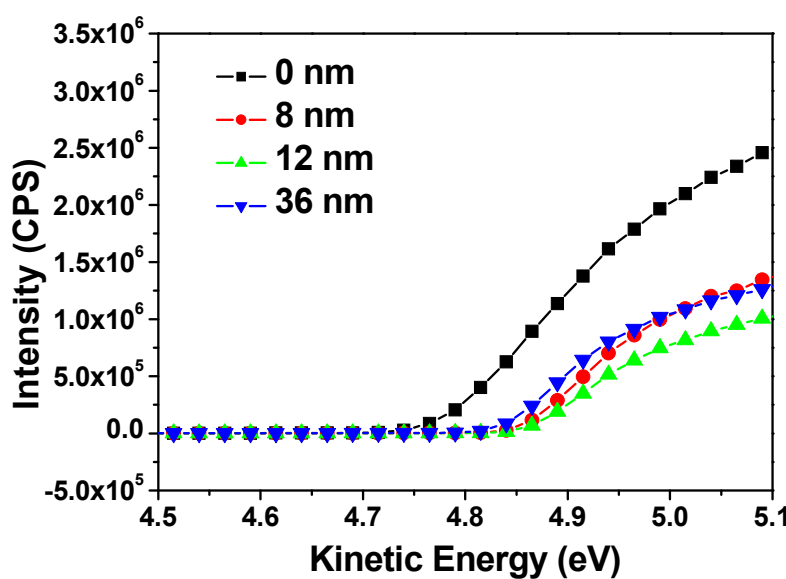


**Fig. S2** Ultraviolet photoelectron spectroscopy measurements of unmodified ITO and ITO modified with 8 nm, 12 nm and 36 nm of P3CPenT. Work functions are extracted from the onset.

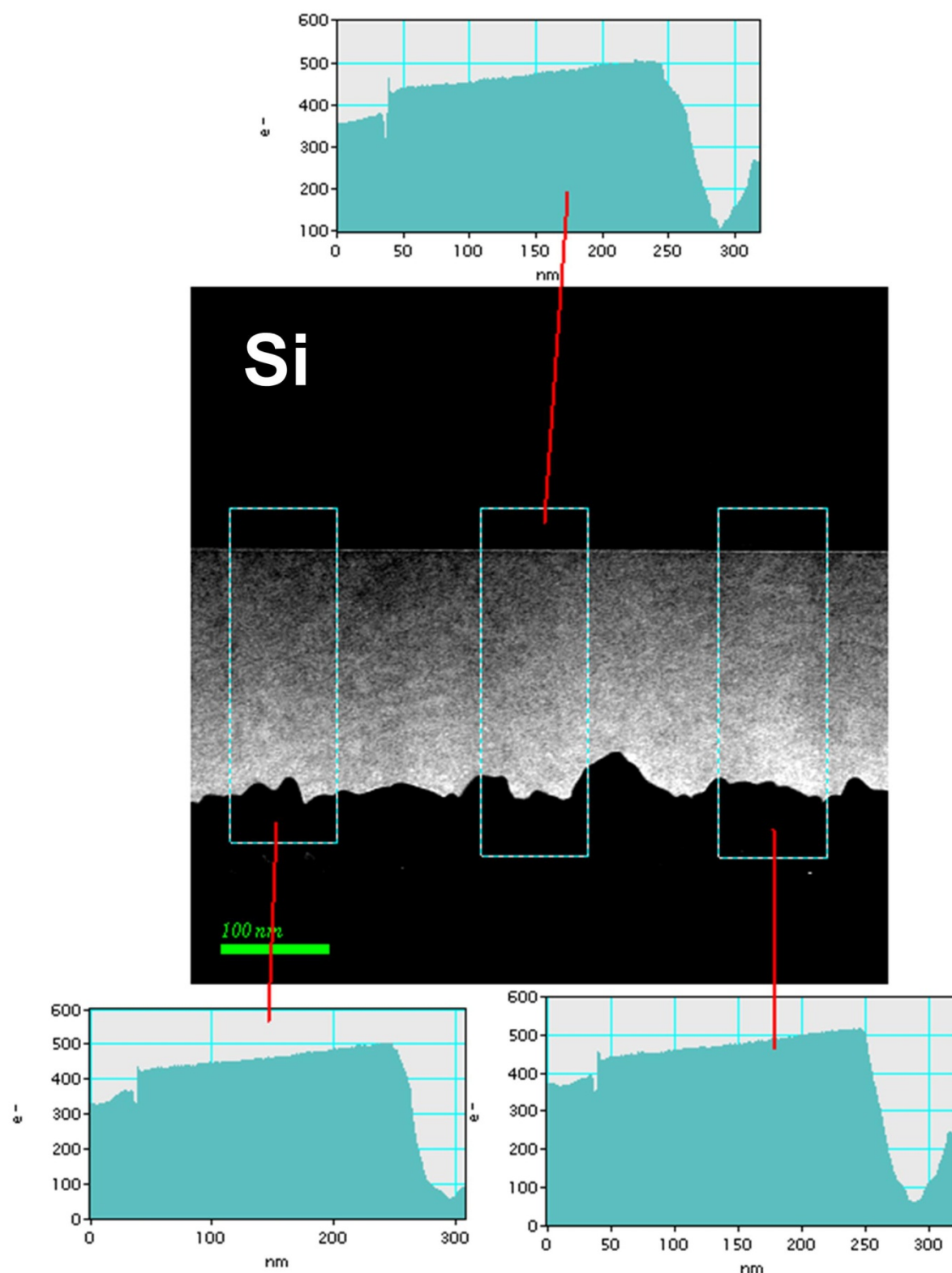


**Fig. S3** Large area cross sectional TEM images of samples with the following architecture: Si/P3HT:PCBM. Plots indicating the average pixel brightness within each rectangular area, which is related to chemical composition, are also included. The scale bars are 100 nm.

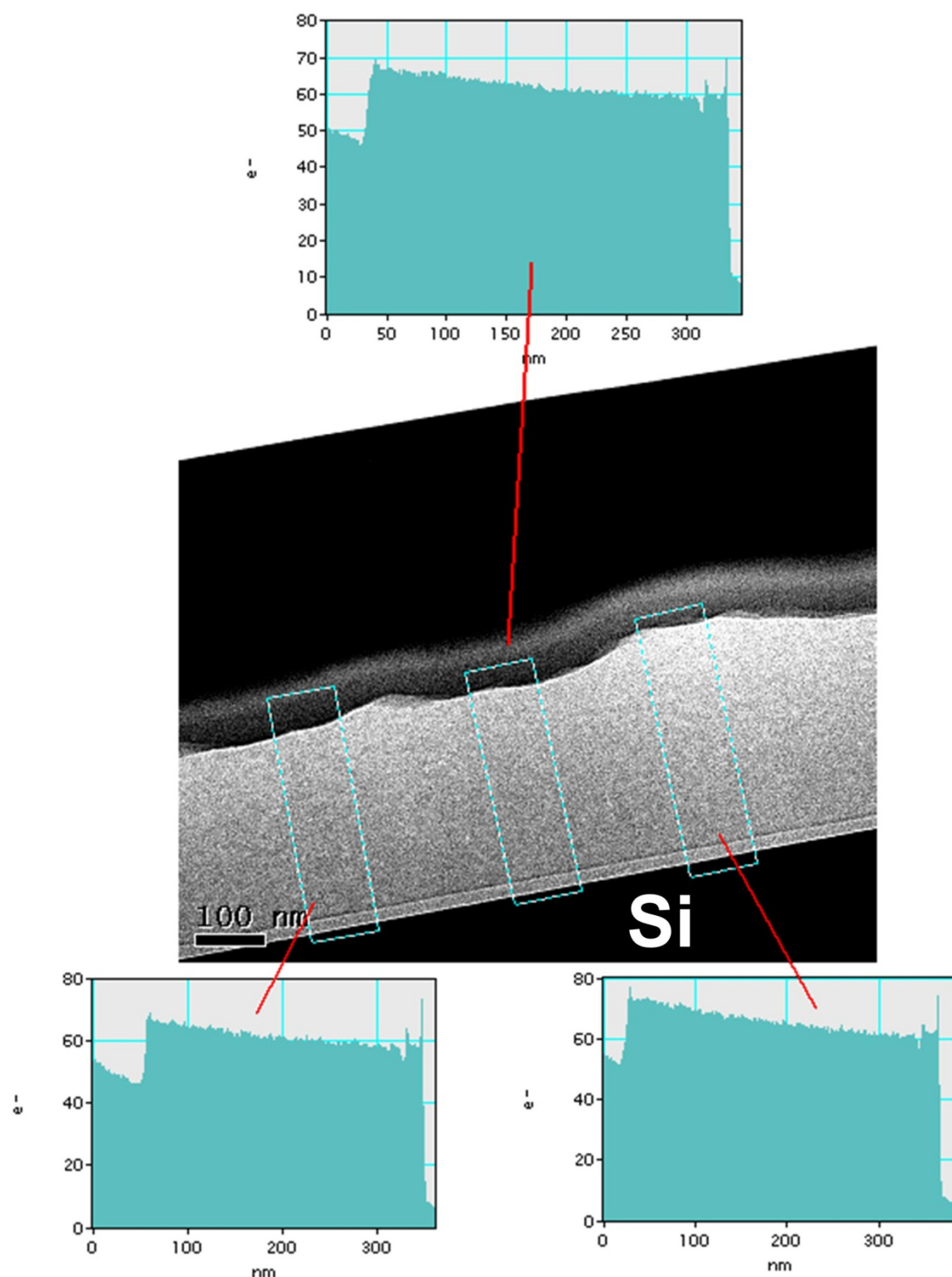


**Fig. S4** Large area cross sectional TEM images of samples with the following architecture: Si/PEDOT:PSS/P3HT:PCBM. Plots indicating the average pixel brightness within each rectangular area, which is related to chemical composition, are also included. The scale bars are 100 nm.

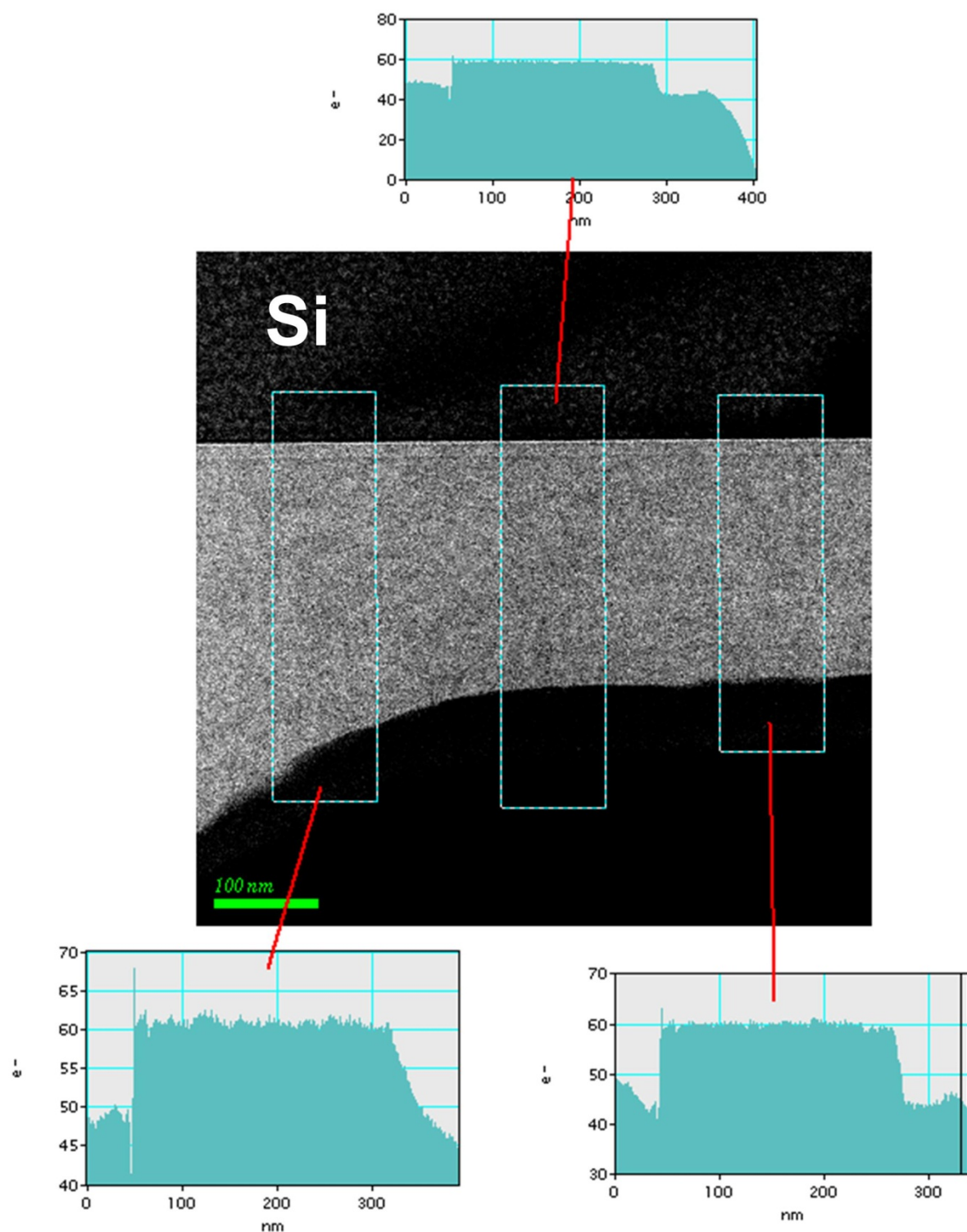


**Fig. S5** Large area cross sectional TEM images of samples with the following architecture: Si/P3CPenT/P3HT:PCBM. Plots indicating the average pixel brightness within each rectangular area, which is related to chemical composition, are also included. The scale bars are 100 nm.

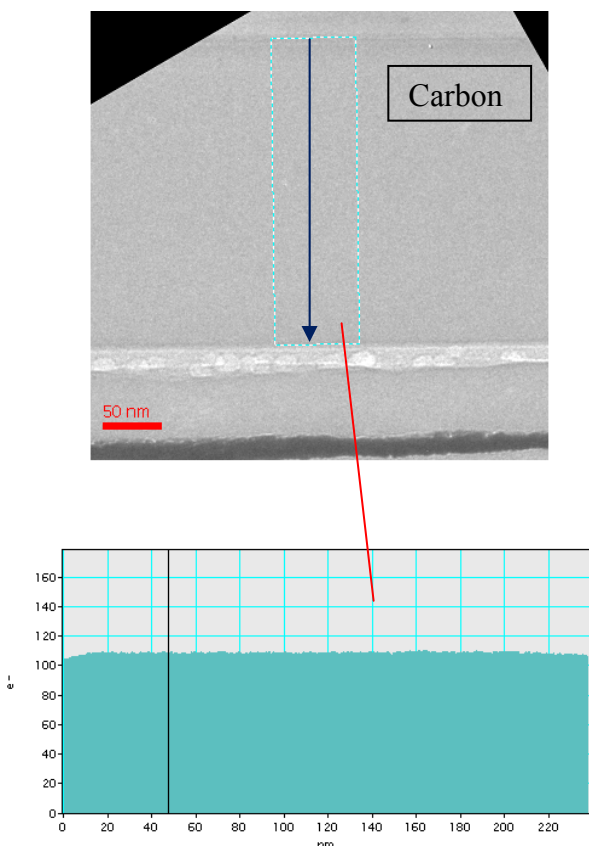


**Fig. S6** A cross sectional TEM image of a thin carbon sample which was prepared for microscopy under the same focussed ion beam conditions as the P3HT:PCBM samples shown in Figure 6 of the main text and Figure S2-S4 in this supporting information section. The TEM signal intensity profile across the carbon film is also included, and the uniform profile indicates a uniform thickness of the carbon film as prepared in the FIB instrument.

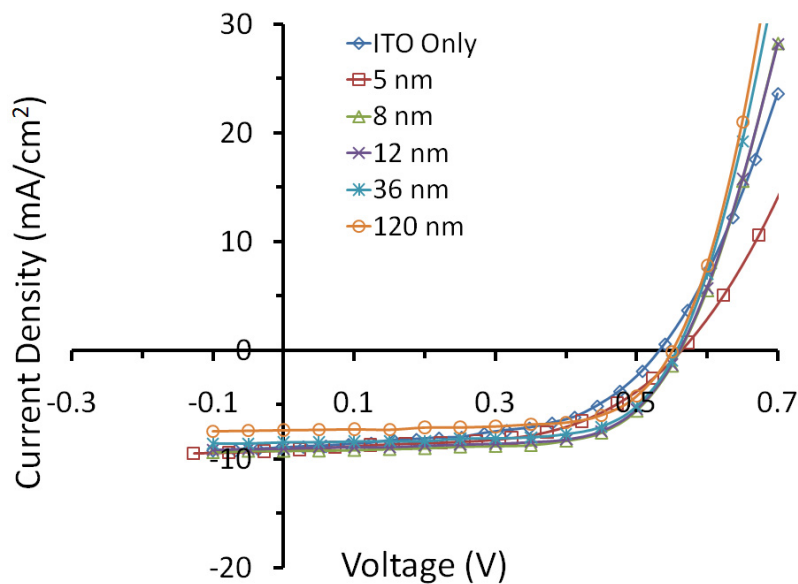


**Fig. S7** Current density-voltage curves for P3HT:PCBM PSCs fabricated with different thicknesses of P3CPenT as an HTL and illuminated with 100 mW/cm<sup>2</sup> simulated solar irradiation.

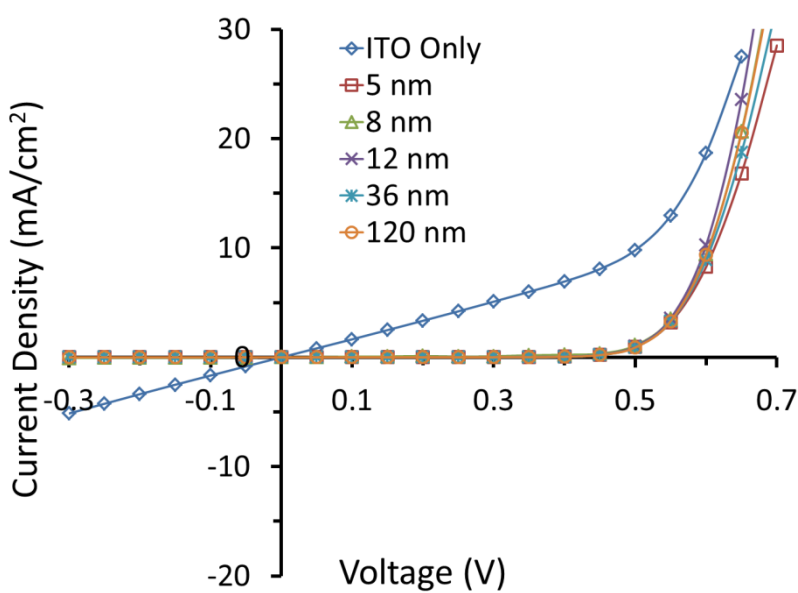
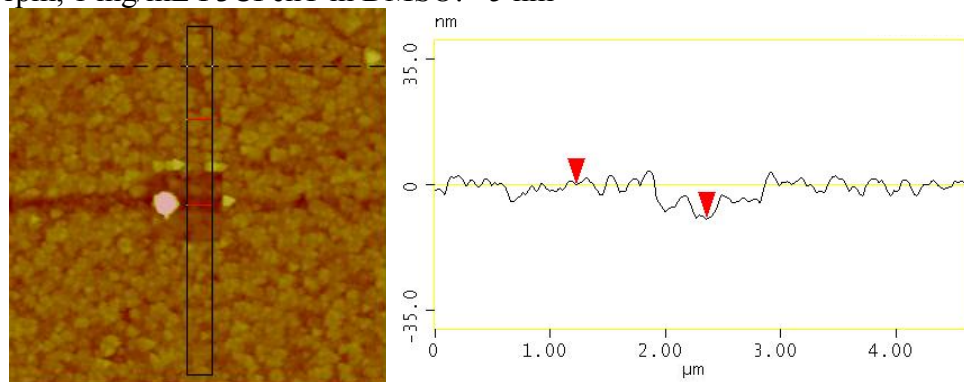
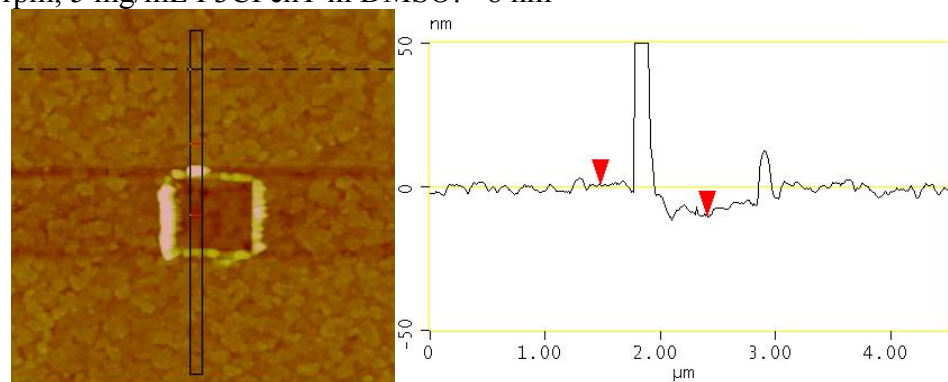


**Fig. S8** Current density-voltage curves for unilluminated P3HT:PCBM PSCs fabricated with different thicknesses of P3CPenT as HTL.

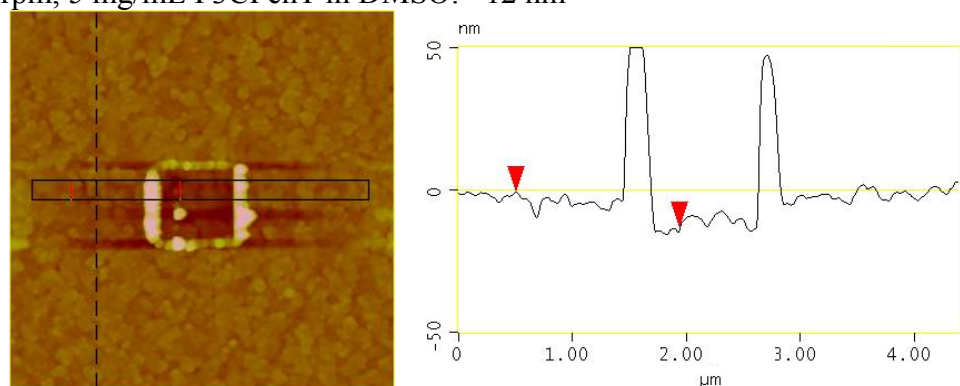
(a) 3000 rpm, 1 mg/mL P3CPenT in DMSO: ~5 nm



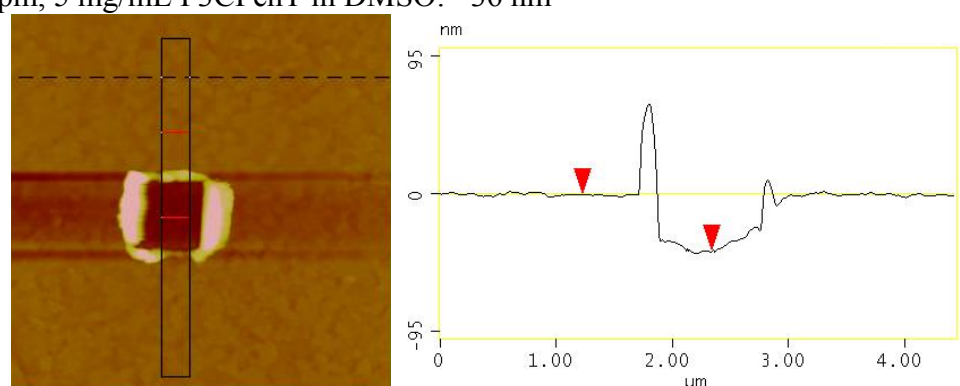
(b) 3000 rpm, 5 mg/mL P3CPenT in DMSO: ~8 nm



(c) 2000 rpm, 5 mg/mL P3CPenT in DMSO: ~12 nm



(d) 600 rpm, 5 mg/mL P3CPenT in DMSO: ~36 nm



(e) 1000 rpm, 15 mg/mL P3CPenT in DMSO: ~120 nm

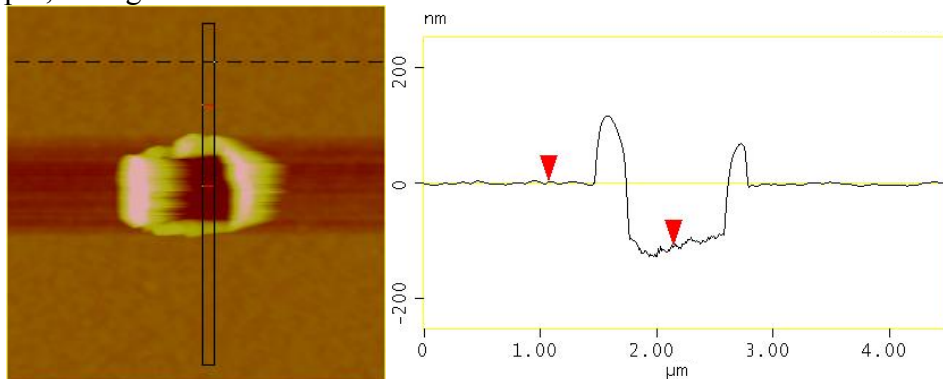


**Fig. S9** Determination of the average thickness of P3CPenT deposited on ITO surfaces by AFM. In (a), spin casting at 3000 rpm with 1 mg/mL P3CPenT in DMSO is found to lead to film thicknesses of ~5 nm, in (b), spin casting at 3000 rpm with 5 mg/mL P3CPenT in DMSO is found to lead to film thicknesses of ~8 nm, in (c), spin casting at 2000 rpm with 5 mg/mL P3CPenT in DMSO is found to lead to film thicknesses of ~12 nm, in (d), spin casting at 600 rpm with 5 mg/mL P3CPenT in DMSO is found to lead to film thicknesses of ~36 nm, and in (e), spin casting at 1000 rpm with 15 mg/mL P3CPenT in DMSO is found to lead to film thicknesses of ~120 nm. The red triangles were generated in the AFM analysis software, but were not used in the determination of thickness. In each panel, the AFM image dimensions are 5  $\mu\text{m}$  x 5  $\mu\text{m}$ .

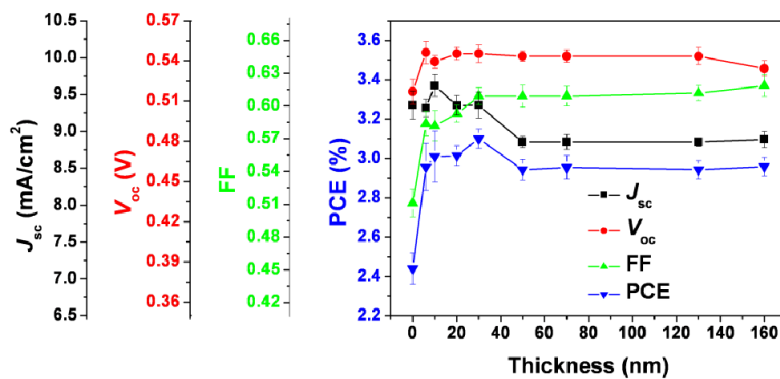


**Fig. S10** Influence of PEDOT:PSS HTL thickness over P3HT:PCBM device performance. Each point represents the average of 4 PV devices.

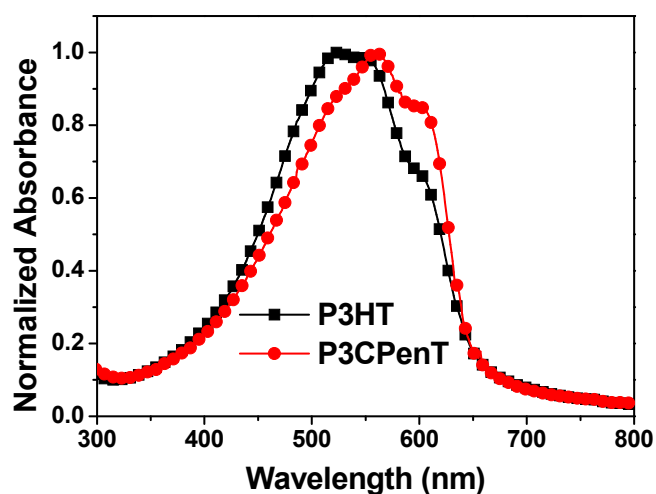


**Fig. S11** Normalized absorption spectra of P3HT and P3CPenT films.

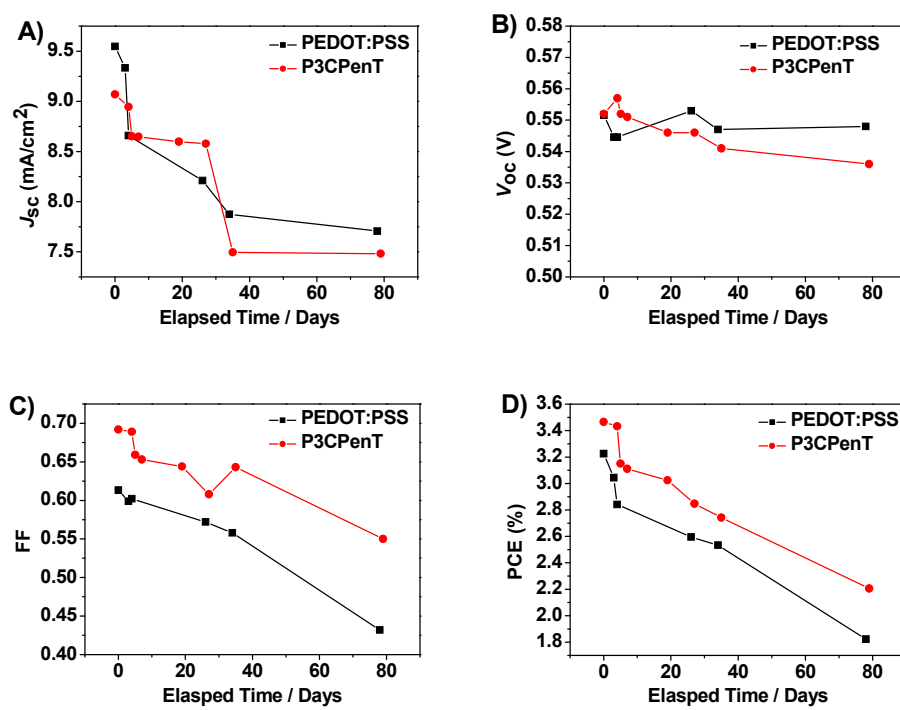


**Fig. S12** Degradation of photovoltaic parameters for P3HT:PCBM BHJ devices fabricated with PEDOT:PSS (30 nm) or P3CPenT (12 nm) as an HTL. A)  $J_{sc}$ ; B)  $V_{oc}$ ; C) FF and D) PCE.

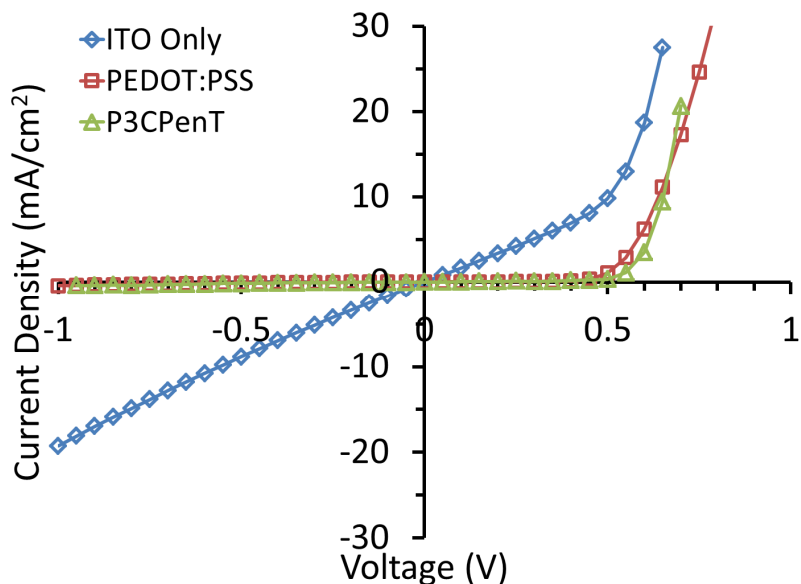


**Fig. S13** Current density-voltage curves for unilluminated P3HT:PCBM PSCs fabricated with different hole transport layers including ITO only, PEDOT:PSS and P3CPenT NWs.

**Table S1** Summarized contact angles of Si substrates modified by PEDOT:PSS or P3CPenT.

	Water contact angle (°)	<i>n</i> -Hexadecane contact angle (°)	Surface energy (mJ/m <sup>2</sup> )
Unmodified Si	9	9	72
Si modified by PEDOT:PSS	4	10	73
Si modified by P3CPenT	47	4	54

**Table S2** The average (over nine devices) photovoltaic performance of PSCs made with P3CPenT HTLs cast from DMSO and pyridine. For DMSO-casting, a 5 mg/mL solution was spin-cast at 1000 rpm, and for pyridine-casting, a 2.5 mg/mL solution was spin-cast at 3000 rpm, both for 5 minutes. The resulting P3CPenT films were both measured via ellipsometry to be 11 nm thick. All HTL spin-casting was done at 90 °C, and the samples were annealed subsequently in air at 90 °C.

Casting Solution	$J_{sc}$ (mA/cm <sup>2</sup> )	$V_{oc}$ (V)	FF	PCE (%)	$R_s$ ( $\Omega$ cm <sup>2</sup> )	$R_{sh}$ ( $k\Omega$ cm <sup>2</sup> )
DMSO	7.62 (0.40)	0.58 (0.004)	0.60 (0.01)	2.67 (0.12)	6.65 (0.67)	0.71 (0.13)
	6.57 (0.34)	0.57 (0.003)	0.58 (0.02)	2.17 (0.09)	7.76 (0.63)	0.58 (0.23)
Pyridine						

**Table S3** Average photovoltaic parameters of devices fabricated with various HTLs: only ITO, PEDOT:PSS (30 nm), P3CPenT (8 nm) and dip-cast P3CPenT. Standard deviations are included in parentheses. The fourth entry confirms that PSCs based on P3CPenT HTLs formed by dip-casting/absorption methods are also functional.

HTL	J <sub>sc</sub> (mA/cm <sup>2</sup> )	V <sub>oc</sub> (V)	FF	PCE (%)	R <sub>s</sub> (Ω cm <sup>2</sup> )	R <sub>sh</sub> (kΩ cm <sup>2</sup> )	Best PCE (%)
Only ITO	9.24 (0.16)	0.52 (0.01)	0.51 (0.01)	2.44 (0.1)	6.03 (0.12)	0.34 (0.09)	2.5
	PEDOT:PSS	9.24 (0.09)	0.55 (0.003)	0.61 (0.006)	3.1 (0.13)	8.17 (0.14)	1.78 (0.03)
P3CPenT	9.26 (0.18)	0.56 (0.002)	0.67 (0.006)	3.42 (0.12)	6.45 (0.20)	1.81 (0.04)	3.7
P3CPenT*	9.17 (0.06)	0.56 (0.005)	0.60 (0.005)	3.06 (0.06)	6.73 (0.17)	1.79 (0.13)	3.1

\* This P3CPenT layer was formed by immersing an ITO-coated substrate into P3CPenT solution (DMSO) as described in the experimental section.

## References

- S1 D. K. Owens and R. C. Wendt, *J. Appl. Polym. Sci.*, 1969, **13**, 1741.  
S2 B. Jańczuk and E. Chibowski, *J. Coll. Inter. Sci.*, 1983, **95**, 268.